

Synchrotron radiation-based irradiance calibration from 200 to 400 nm at the Synchrotron Ultraviolet Radiation Facility III

Ping-Shine Shaw, Uwe Arp, Robert D. Saunders, Dong-Joo Shin, Howard W. Yoon, Charles E. Gibson, Zhigang Li, Albert C. Parr, and Keith R. Lykke

A new facility for measuring irradiance in the UV was commissioned recently at the National Institute of Standards and Technology (NIST). The facility uses the calculable radiation from the Synchrotron Ultraviolet Radiation Facility as the primary standard. To measure the irradiance from a source under test, an integrating sphere spectrometer–detector system measures both the source under test and the synchrotron radiation sequentially, and the irradiance from the source under test can be determined. In particular, we discuss the calibration of deuterium lamps using this facility from 200 to 400 nm. This facility improves the current NIST UV irradiance scale to a relative measurement uncertainty of 1.2% ($k = 2$). © 2007 Optical Society of America

OCIS codes: 120.5630, 120.4800, 260.7190.

1. Introduction

Source calibration and detector calibration are the two main pillars in the field of optical radiometry.¹ The radiation scale used for each of the calibrations is derived from a primary standard, and the scale is disseminated through the calibration chain by using transfer standards. In source calibration, blackbody sources have a long history of being used as primary radiance standards. In 1960, tungsten ribbon–filament lamps calibrated with blackbodies were used as transfer standards for radiance calibration² at the National Institute of Standards and Technology (NIST, formerly known as the National Bureau of Standards). Subsequently, in 1963, NIST established an irradiance scale³ based on its radiance scale to wavelengths above 250 nm using quartz–iodine lamps as transfer standards. However, the scale for the UV region below 250 nm could not be realized by using blackbody sources because of their

low flux and sharp drop off in this spectral region. A large variation in radiant flux across this UV region significantly increases measurement uncertainty caused by scattered light and nonlinearity problems in the detection system. To achieve increased and spectrally flat radiant flux below 250 nm, the blackbody source must be operated at such a high temperature that is difficult if not impossible to achieve.

As the demands for calibration deep into the UV increased over the years, there was considerable effort in developing new primary standards for UV and vacuum UV (VUV) including plasma sources (i.e., wall-stabilized hydrogen and blackbody arcs)^{4–7} and synchrotron radiation.^{8–12} Because of the relative ease of operation, the NIST scale in the UV and VUV was first established by Ott *et al.*^{4,5} using the hydrogen arc discharge in 1975. This scale, along with the scale based on a blackbody at longer wavelengths, is still being used today at the NIST Facility for Automated Spectroradiometric Calibrations (FASCAL)^{13,14} for irradiance calibrations of deuterium lamps from 200 to 400 nm.

Synchrotron radiation, on the other hand, was recognized as an absolute radiation standard by Tomboulian and Hartman⁸ in the early days of dedicated synchrotron machines. Just as blackbody radiation is calculable by the Planck equation, the characteristics of synchrotron radiation are calculable by the Schwinger equation.¹⁵ Most importantly, in the UV and shorter wavelength regions, synchro-

The authors are with the National Institute of Standards and Technology, Gaithersburg, Maryland 20899. D.-J. Shin is also with the Korea Research Institute of Standards and Science, Yuseong, Daejeon 305-600, South Korea. P.-S. Shaw's e-mail address is shaw@nist.gov.

Received 26 April 2006; revised 24 July 2006; accepted 17 August 2006; posted 7 September 2006 (Doc. ID 70284); published 15 December 2006.

0003-6935/06/010025-11\$15.00/0

© 2007 Optical Society of America

tron radiation emitted from a storage ring has the highest accuracy in calculable irradiance among all known radiation standards to date. Synchrotron radiation as a primary irradiance standard for a broad spectral range from x rays to infrared has since been established at several synchrotron facilities around the world including the NIST Synchrotron Ultraviolet Radiation Facility (SURF) in the United States,^{9,16} the Glasgow University 340 MeV synchrotron and the Daresbury 5 GeV machine in the UK,¹⁷ the 750 MeV Tsukuba Electron Ring for Accelerating and Storage (TERAS) in Japan,¹⁸ and the 6 GeV Deutsches Elektronen Synchrotron (DESY)^{11,12} and the electron storage ring of the Berliner Elektronen Speicherring-Gesellschaft für Synchrotronstrahlung (BESSY) in Germany.^{19–21} However, despite all the promises of a primary standard source, the development of radiometric synchrotron sources was relatively slow, mainly because of the limited synchrotron facilities available and the evolving technologies in quantifying synchrotron parameters that are crucial for the calculability of synchrotron radiation.

At the NIST, the SURF was first used as an absolute VUV source in the 1970s,¹⁶ although determination of the electron beam current relied on a spectrometer system calibrated by using the NIST irradiance standard at that time. Only after a technique was developed to measure the beam current based on electron counting in the early 1980s^{22,23} did the SURF become an independent primary source standard, and the SURF-based irradiance scale was compared with blackbody and silicon photodiode scales at 600 nm.²⁴ Soon after, the comparison moved to the UV where a few wavelengths were compared with other irradiance transfer standards such as quartz–tungsten halogen lamps and argon miniarcs.^{25,26} A more thorough irradiance scale comparison was performed in 1998 from 210 to 300 nm on SURF II.²⁷ In 2000, SURF II was upgraded to SURF III as a dedicated synchrotron radiation facility for radiometry.²⁸ The new SURF III has a much more uniform magnetic field and a more stable electron beam. The electron beam current can be varied from more than 300 mA to a single electron in the beam (corresponding to a 9.1 pA beam current), which provides a variable radiation flux extending over 10 orders of magnitude. The electron energy is tunable from 50 to 380 MeV. With this improved synchrotron facility, we recently constructed and commissioned the Facility for Irradiance Calibration Using Synchrotrons (FICUS) where sources can be calibrated against a new synchrotron-radiation-based NIST irradiance standard from 200 to 400 nm.

The FICUS is based on a new white-light beamline at SURF III.^{29,30} The beamline directs the calculable SURF III radiation to the user station with minimum obstruction from optical components. To reduce measurement uncertainty, no mirrors are used and only one window separates the synchrotron source and the spectrometer–detector system. The transmission of the window can be measured directly on the beamline instead of requiring the removal of the window for transmission measurement elsewhere. The irradi-

ance from a device under test (DUT) or a transfer standard can be compared directly with synchrotron radiation. Here we discuss the design and operation of the FICUS. The realization of an irradiance scale using synchrotron radiation is described. We present a detailed discussion on the calibration of a new generation of stable deuterium lamps as transfer standards from 200 to 400 nm where the estimated relative uncertainty is 1.2% at a coverage factor of $k = 2$ (i.e., an approximately 95% confidence level¹), which is a significant improvement over the current UV irradiance scale of the NIST.

2. Principle of Synchrotron-Radiation-Based Irradiance Calibration

The characteristics of synchrotron radiation can be accurately determined based on Schwinger's equation, which expresses the radiant flux $\Phi_{\lambda,SR}$ emitted by a relativistic charge e into a solid angle $d\Omega$ at a wavelength interval of $d\lambda$ as³¹

$$\frac{d^2\Phi_{\lambda,SR}}{d\lambda d\Omega} = \frac{27e^2}{32\pi^3\rho^2} \left(\frac{\lambda_c}{\lambda}\right)^4 \gamma^8 (1 + \gamma^2\psi^2)^2 \times \left[K_{2/3}^2(z) + \frac{\gamma^2\psi^2}{1 + \gamma^2\psi^2} K_{1/3}^2(z) \right], \quad (1)$$

with

$$z = \frac{1}{2} \frac{\lambda_c}{\lambda} (1 + \gamma^2\psi^2)^{3/2},$$

where ρ is the radius of curvature of the electron's orbit, ψ is the observer's angle above or below the orbital plane, $K_{2/3}$ and $K_{1/3}$ are modified Bessel functions, and λ_c is the critical wavelength defined as

$$\lambda_c = \frac{4\pi\rho}{3\gamma^3}, \quad \gamma = \frac{E_e}{m_e c^2},$$

where E_e is the electron energy, m_e is the rest mass of the electron, and c is the speed of light. The two modified Bessel functions at the right-hand side of Eq. (1) represent the contributions from horizontal and vertical polarizations, respectively. At $\psi = 0$, the term for vertical polarization vanishes, and the radiation is linearly polarized in the horizontal direction.

To calibrate a light source using synchrotron radiation, a spectrometer–detector system with a defining aperture is used to measure two sources alternately. For the measurement of synchrotron radiation, the defining aperture, with an area A , faces the incident synchrotron radiation at a distance d from the tangent point of the storage ring. Using Eq. (1) the spectral irradiance $E_{\lambda,SR}$ of synchrotron radiation entering this aperture can be expressed as

$$E_{\lambda,SR}(\lambda) = \frac{1}{A} \left(\frac{I_{SR}}{d^2} \int \int_A \frac{d^2\Phi_{\lambda,SR}}{d\Omega d\lambda} dx dy \right), \quad (2)$$

where I_{SR} is the electron beam current in the storage ring, and the surface integral is over area A of the aperture. The spectral irradiance $E_{\lambda,SR}$ is completely determined given three storage parameters: the electron beam current I_{SR} , the orbital radius ρ , and the electron energy E_e (or the applied magnetic field), along with the geometric parameters of the aperture, d and A . For a typical measurement setup, the defining aperture of the detector system, with an area of the order of 1 cm^2 and a distance d close to 700 cm , is placed at an angle $\psi = 0$. In this configuration, the aperture subtends a very small angle (of the order of 1 mrad) for synchrotron radiation. At $\psi = 0$, the non-uniformity of radiation in the aperture is rather small and the variation of $E_{\lambda,SR}$ over area A is small. In the case of the FICUS, for example, calculation shows that, at 380 MeV of electron energy, the variation in $E_{\lambda,SR}$ is approximately only 1% for any circular aperture with a diameter less than 1 cm . An accurate determination of A is generally not required.

For a detector system operating in air, a window must be used to maintain vacuum in the storage ring. By inserting a window in the optical path, the expression for spectral irradiance becomes

$$E_{\lambda,SR}(\lambda) = \frac{T(\lambda)}{A} \left(\frac{I_{SR}}{d^2} \int \int_A \frac{d^2\Phi_{\lambda,SR}}{d\Omega d\lambda} dx dy \right), \quad (3)$$

where $T(\lambda)$ is the transmission of the window at wavelength λ .

With the spectral irradiance at the aperture known from Eq. (3) by numerical calculation, one can, in principle, use the signal from the detector to determine the responsivity of the spectrometer–detector system, which, in turn, can be used to calibrate any radiation source. However, in practice, the situation is complicated by the stray light or spectral scattering of radiation in the spectrometer–detector system. The algorithm for stray-light correction was developed previously.^{32–34} Following Ref. 32, the relation between the measured signal and the spectral irradiance is given by

$$S(\lambda_0) = \int R(\lambda_0, \lambda) E_{\lambda}(\lambda) d\lambda, \quad (4)$$

where $S(\lambda_0)$ is the signal measured with the spectrometer set at wavelength λ_0 , and $R(\lambda_0, \lambda)$ is the responsivity function of the spectrometer–detector system. The responsivity function is usually expressed as the product of the responsivity of the system at λ_0 , $r(\lambda_0)$, and the slit-scattering function, $z(\lambda_0, \lambda)$. Equation (4) then becomes

$$S(\lambda_0) = r(\lambda_0) \int z(\lambda_0, \lambda) E_{\lambda}(\lambda) d\lambda. \quad (5)$$

The slit-scattering function $z(\lambda_0, \lambda)$ has a peak value of unity when $\lambda = \lambda_0$ and diminishes rapidly with an increased difference between λ_0 and λ . The slit-scattering function can be readily measured by using a tunable laser as was performed for this work and discussed in Section 4.

To deduce the spectral irradiance from the measured signal in Eq. (5) one can treat the stray-light contribution as a small perturbation and use an iterative technique. To start, an approximate solution, $E_{\lambda}(\lambda_0)^{(0)}$, for $E_{\lambda}(\lambda_0)$ in Eq. (5) is given by

$$E_{\lambda}(\lambda_0)^{(0)} = \frac{1}{r(\lambda_0)} \frac{S(\lambda_0)}{\int z(\lambda_0, \lambda) d\lambda},$$

where we assumed $E_{\lambda}(\lambda)$ to be essentially constant around wavelength λ_0 , and the term can be removed from the integral in Eq. (5). Substituting the above expression into the right-hand side of Eq. (5) and defining the result of the integral as $S(\lambda_0)^{(0)}$, we have

$$S(\lambda_0)^{(0)} = \int z(\lambda_0, \lambda) [r(\lambda_0) E_{\lambda}(\lambda)^{(0)}] d\lambda. \quad (6)$$

Note that because $r(\lambda_0) E_{\lambda}(\lambda_0)^{(0)}$ does not depend on $r(\lambda_0)$, the calculation of $S(\lambda_0)^{(0)}$ from the above equation requires only the measured signal and the slit-scattering function. Once $S(\lambda_0)^{(0)}$ is known, the difference between $S(\lambda_0)$ and $S(\lambda_0)^{(0)}$ can be used to find the correction term, $\Delta E_{\lambda}(\lambda_0)^{(0)}$, for $E_{\lambda}(\lambda_0)^{(0)}$ from

$$S(\lambda_0) - S(\lambda_0)^{(0)} = \int z(\lambda_0, \lambda) [r(\lambda_0) \Delta E_{\lambda}(\lambda)^{(0)}] d\lambda.$$

As before, an approximate solution for $\Delta E_{\lambda}(\lambda_0)^{(0)}$ is

$$\Delta E_{\lambda}(\lambda_0)^{(0)} = \frac{1}{r(\lambda_0)} \frac{S(\lambda_0) - S(\lambda_0)^{(0)}}{\int z(\lambda_0, \lambda) d\lambda}.$$

With this correction term, the improved solution for the spectral irradiance becomes

$$E_{\lambda}(\lambda_0)^{(1)} = \frac{1}{r(\lambda_0)} \frac{2S(\lambda_0) - S(\lambda_0)^{(0)}}{\int z(\lambda_0, \lambda) d\lambda}.$$

Repeating this process by substituting the above solution back to the right-hand side of Eq. (5), we define

$$S^{(1)}(\lambda_0) = \int z(\lambda_0, \lambda) [r(\lambda) E_\lambda(\lambda)^{(1)}] d\lambda, \quad (7)$$

and the approximate solution to the correction term of $E_\lambda(\lambda_0)^{(1)}$ is

$$\Delta E_\lambda(\lambda_0)^{(1)} = \frac{1}{r(\lambda_0)} \frac{S(\lambda_0) - S(\lambda_0)^{(1)}}{\int z(\lambda_0, \lambda) d\lambda}.$$

The solution to $E_\lambda(\lambda_0)$ with second-order correction is given by

$$E_\lambda(\lambda_0)^{(2)} = \frac{1}{r(\lambda_0)} \frac{3S(\lambda_0) - S(\lambda_0)^{(0)} - S(\lambda_0)^{(1)}}{\int z(\lambda_0, \lambda) d\lambda}, \quad (8)$$

where $S(\lambda_0)^{(0)}$ and $S(\lambda_0)^{(1)}$ can be calculated by using Eqs. (6) and (7). In general, as in this work, the solution with two iterations is accurate enough for all practical purposes.

To calibrate the spectral irradiance of the radiation from a source, the spectrometer–detector system is first exposed to synchrotron radiation for a spectral scan with measured signal $S_{\text{SR}}(\lambda)$. Subsequently, the spectrometer–detector system is exposed to the DUT source, and the measured signal is $S_{\text{DUT}}(\lambda)$. Then the measurement equation for the spectral irradiance of the DUT source, $E_{\lambda, \text{DUT}}(\lambda)$, can be expressed by using the stray-light reduction algorithm of Eq. (8) as

$$E_{\lambda, \text{DUT}}(\lambda_0) = \frac{3S_{\text{DUT}}(\lambda_0) - S_{\text{DUT}}(\lambda_0)^{(0)} - S_{\text{DUT}}(\lambda_0)^{(1)}}{3S_{\text{SR}}(\lambda_0) - S_{\text{SR}}(\lambda_0)^{(0)} - S_{\text{SR}}(\lambda_0)^{(1)}} \times \left(\frac{T(\lambda_0)}{A} \frac{I_{\text{SR}}}{d^2} \int \int_A \frac{d^2\Phi_{\lambda, \text{SR}}}{d\Omega d\lambda} dx dy \right), \quad (9)$$

where we used Eq. (3) for the calculated spectral irradiance from synchrotron radiation, and the integrand of the surface integral is the direct substitution of the Schwinger equation.

3. Description of the Calibration Facility

The FICUS, as shown in Fig. 1, consists of four main components: SURF III generating synchrotron radiation as an irradiance standard, a white-light beamline to transport synchrotron radiation, a spectrometer and detector system for comparing radiation from SURF III and the DUT sources, and a platform for mounting the DUT sources. At present, the radiation detection and the DUT source are operated in air. An UV window at the end of the white-light beamline separates the vacuum of the storage ring and the beamline from air while transmitting radiation into air for detection.

A. SURF III

SURF III is a compact weak-focusing storage ring designed specifically for radiometry covering a wide

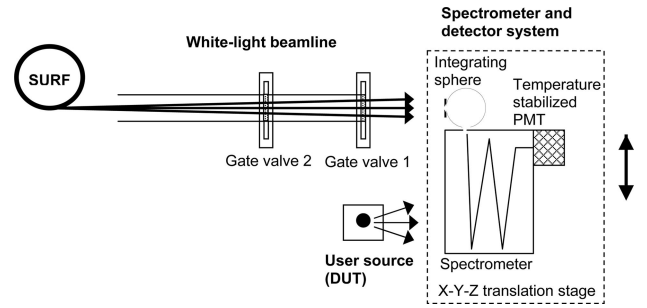


Fig. 1. Schematic of the FICUS for synchrotron-radiation-based irradiance calibration.

spectrum from the far-infrared to the soft x ray.²⁸ A unique single magnet design with high uniformity in the magnetic field facilitates a circular electron orbit with a diameter of 167.6 cm. Low electron energy of up to 380 MeV generates radiation peaked in the extreme UV with reduced x-ray production. A low flux of x rays is particularly important for UV work because of the degradation of optical components such as windows and detectors that are vulnerable to radiation damage.^{35,36} The electron beam has a typical vertical beam size of 30 μm FWHM. With this beam size, no discernible dependence on vertical beam size was observed in irradiance for this work. The lifetime of the electron beam at an electron energy of 380 MeV is of the order of hours and much longer than the several minutes of measurement time for irradiance using our spectrometer. Nevertheless, all the data are normalized by the beam current.

B. White-Light Beamline

As described in detail elsewhere,^{29,30} the beamline where FICUS is based is a white-light beamline approximately 6 m long. Inside the beamline a series of baffles reduce multiple scattering of synchrotron radiation from the stainless steel walls of the beamline. With all the adjustable apertures in the beamline fully open, a full 20 mrad angle of synchrotron radiation can reach the end of the beamline without any obstruction. This large opening allows us to determine and control the effect of optical diffraction, especially at longer wavelengths.

For the FICUS, a fused silica UV window was installed in a vacuum gate valve (gate valve 1 in Fig. 1) at the end of the beamline such that the detection of the synchrotron radiation could be performed in air beyond the end of the beamline. To maintain the calculability of synchrotron radiation, the transmission of the window must be accurately determined. For this, a second fused silica window was installed in a second gate valve (gate valve 2 in Fig. 1) to maintain the vacuum integrity of the beamline and the storage ring during transmittance measurements. The transmission of the first window can be derived from two measurements of the synchrotron radiation exiting from the beamline by using the spectrometer–detector system: one with the first window in the

beam path and one with the window out of the beam path. Because both windows are mounted in gate valves, they can be positioned in and out of the synchrotron beam reproducibly.

The advantage of this technique for transmittance measurement is that the UV window does not need to be removed from the beamline to have its transmittance measured at other facilities. More importantly, the beam used for the transmission measurement is the same as the beam used for actual calibration. This ensures that the measured transmittance is for a region on the window and at an incident angle that is identical to the synchrotron beam during calibration, thus eliminating the uncertainty associated with removing the window for transmittance measurement at another location.²⁷

C. Spectrometer-Detector System

The spectrometer of the FICUS is a 0.25 m grating spectrometer with a thermoelectric-cooled bialkali photomultiplier tube (PMT) attached to the exit slit. The bialkali PMT was chosen for its low noise and long-term stability. The resolution of the spectrometer was set at 5 nm, which was confirmed by scanning the 254 nm line of a calibration mercury lamp as shown in Fig. 2. The current from the PMT was converted to voltage using a current-to-voltage preamplifier and recorded by a computer through a digital voltmeter.

At the entrance slit of the spectrometer, a polytetrafluoroethylene (PTFE) integrating sphere with a circular entrance aperture (0.95 cm in diameter) was used to collect radiation. The integrating sphere was used to diffuse and depolarize incident radiation to compensate for the differences in polarization and geometry of the incident radiation. Without an integrating sphere, the radiation throughput of the spectrometer could be affected by these differences, thus resulting in errors in calibration. Typically, a DUT source, such as a deuterium lamp, is unpolarized and measured at a distance of the order of 50 cm while the

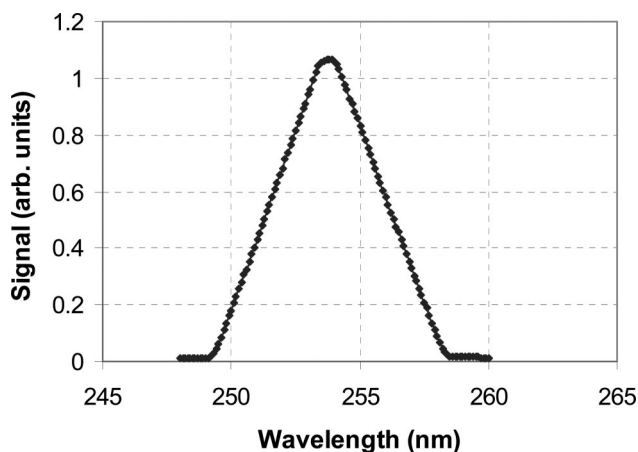


Fig. 2. Scanning of the 0.25 m spectrometer across the 253.7 nm mercury line from a calibration mercury lamp.

synchrotron radiation is highly polarized and measured at a distance of several meters.

The whole spectrometer and detector system is mounted on an x - y translation stage such that the system can be moved to measure synchrotron radiation exiting from the end of the beamline or the radiation from a DUT source. The positioning of the spectrometer and detector system to each source is aligned with lasers. The movements of the x - y stage are controlled by a computer to ensure repeatable positioning and automation of the entire measurement.

D. Platform for Device Under Test Sources

The DUT source to be calibrated against synchrotron radiation is placed on a platform next to the white-light beamline. The source is mounted on a translation stage that allows fine adjustment of the distance between the DUT source and the entrance aperture of the integrating sphere. An alignment laser that traces the center and normal direction of the entrance aperture is used to position a DUT source on the platform.

4. Establishment of Irradiance Standard Using Synchrotron Radiation

Following the measurement equation of Eq. (9), spectral irradiance calibration requires accurate knowledge of several parameters. For synchrotron radiation, the spectral irradiance is calculated from the electron beam storage parameters of electron energy, the orbital radius, the beam current and geometric parameters of the distance of the defining aperture to the tangent point of the electron beam orbit, the window transmission, and the area of the aperture. The calculability of the synchrotron radiation at SURF III was recently validated by scanning the angular distribution of synchrotron radiation by using a set of well-calibrated filter radiometers.³⁷ Good agreement was found between measurement and calculation.

Finally, the measurement equation also makes use of the slit-scattering function of the spectrometer-detector system if stray light cannot be ignored. Below, we discuss the determination of all the parameters related to calibration at the FICUS.

A. Storage Ring Parameters

A detailed discussion of the measurements of the SURF III storage ring parameters has been given elsewhere.²⁸ In brief, the SURF III electron energy and orbital radius are derived from the measured magnetic flux density on orbit and the frequency of the driving rf field. Several field probes monitor the on-orbit magnetic field, and the frequency of the rf field is synchronized with a rubidium atomic clock. The overall relative standard uncertainty is 10^{-4} for the electron energy and 10^{-10} for the orbital radius, which correspond to a relative standard uncertainty of the order of 10^{-5} for the calculated spectral irradiance from 200 to 400 nm.

The electron beam current at SURF III is determined optically by a silicon photodiode exposed to synchrotron radiation. To convert the electron beam current from the signal of the silicon photodiode, the signal resulting from a single electron in the ring is determined by observing the quantized decay of the synchrotron radiation associated with the loss of individual electrons. This electron-counting calibration method is performed regularly at SURF III with several thousand or fewer electrons in the SURF ring. A higher electron beam current is determined by extrapolating the signal from a photodiode by using an amplifier with high linearity.³⁸ The estimated relative standard uncertainty in the measured electron beam current is 2×10^{-3} (Refs. 22 and 23). Because the radiant flux of synchrotron radiation is proportional to the electron beam current, the uncertainty of electron beam current translates directly to the radiant flux uncertainty.

B. Distance Measurement

The distance from the emitting point of the synchrotron radiation to the entrance aperture of integrating sphere d was measured independently by two techniques: optical triangulation and direct measurement using a laser range finder.

In optical triangulation, as shown at the top of Fig. 3, a filter radiometer consisting of a silicon photodiode, a 334 nm bandpass filter, and a 500 μm pin-hole, was mounted on the translation stage near the

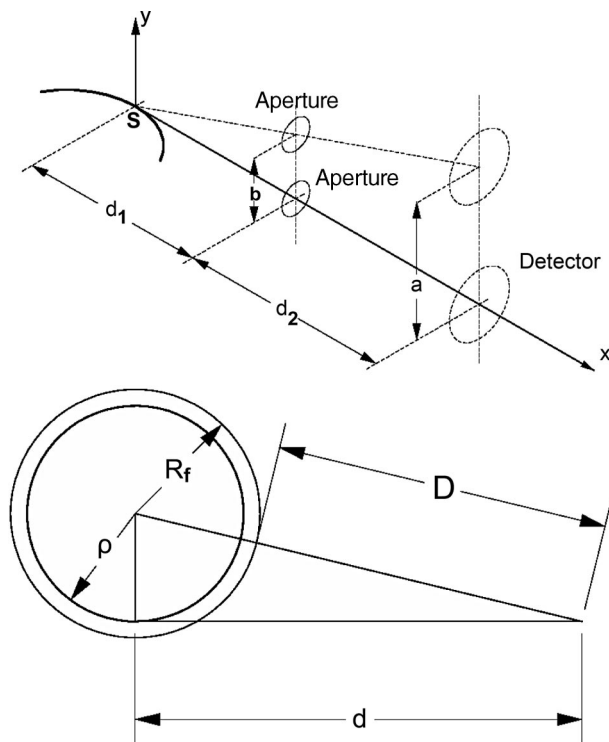


Fig. 3. Schematic for measuring the distance d from the aperture to the tangent point using (top) the triangulation technique where $d = d_1 + d_2$ and (bottom) a fiducial ring (radius R_f) concentric with the electron orbit (radius ρ). The distance D was measured to the shortest distance on the fiducial ring by using a laser range finder.

end of the beamline, approximately 6 m from the tangent point. At approximately 2.5 m from the tangent point, another 1 mm aperture was mounted on a second linear stage. To measure d ($d = d_1 + d_2$ in Fig. 3), the 1 mm aperture was positioned at different vertical positions by its linear stage, and each of their corresponding beam centers at the end chamber was located by the 334 nm filter radiometer. In Fig. 4 there are six scans of the filter radiometer with different positions of the 1 mm aperture. The distance d can be derived by simple geometric consideration as

$$d = \left(\frac{a}{a-b} \right) d_2,$$

where b is the displacement of the 1 mm aperture and a is the corresponding beam center displacement measured by the filter radiometer. The distance between the aperture and the filter radiometer, d_2 , was measured by a laser range finder with an uncertainty better than 1 mm.

The second method to determine distance relies on direct distance measurement using a laser range finder and a fiducial ring around the SURF III storage ring as illustrated at the bottom of Fig. 3. This fiducial ring was carved onto the magnet during the construction of the storage ring and designed with a known radius, R_f , and concentric to the orbit of the electron beam. The shortest distance from the end of the beamline to the fiducial ring, D , was measured using a laser range finder, and, given the electron orbital radius ρ , the distance to the tangent point of the orbit can be determined as

$$d = \sqrt{(R_f + D)^2 - \rho^2}.$$

We found that the measurement results from both techniques agree to within 1 mm out of a distance of more than 6 m. This agrees with the 0.04% estimated relative standard uncertainty on distance measurement.

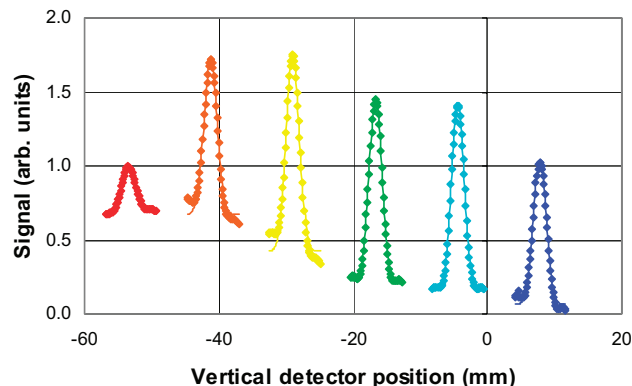


Fig. 4. Signal of vertical scan of the 334 nm filter radiometer for distance measurement. The six scans (in diamonds, from left to right) correspond to measurements with the vertical position of the 1 mm aperture set at 13.10, 18.18, 23.26, 28.34, 33.42, and 38.50 mm. The solid curves are Gaussian fits to measured data to find the centroid of each curve.

C. Window Transmission Measurement

The transmittance of the UV window in gate valve 1 in Fig. 1 can be determined by measuring synchrotron radiation using the spectrometer–detector system with and without the window (i.e., opening and closing gate valve 1) in the path of the radiation. When performing this measurement, the second UV window in gate valve 2 must be closed to maintain a vacuum seal to outside air for the storage ring. With gate valve 2 closed, let $S_{1i}(\lambda)$ and $S_{1o}(\lambda)$ be the signals of synchrotron radiation measured by the spectrometer–detector system with gate valve 1 closed and open, respectively, then the transmittance of the window, $T(\lambda)$, is

$$T(\lambda) = \frac{S_{1i}(\lambda)}{S_{1o}(\lambda)}.$$

Figure 5 shows the typical measured window transmittance from 200 to 400 nm. The transmittance of the window is constantly monitored because the window did show degradation after prolonged exposure to synchrotron radiation. The window was replaced if we deemed the transmission had dropped too much from its original values. However, we found that the transmittance remained unchanged during one round of measurements such as the deuterium lamp calibration, which exposed the window to synchrotron radiation at low SURF current (≈ 15 mA) for a total time of less than half an hour.

Another effect one must consider with a window in the beam path is the lensing effect by the refraction of radiation from a plano–parallel window that makes the tangent point of the beam appear closer than its physical distance. For the FICUS, our calculation shows a 1 mm reduction in the distance because of the presence of the window. While this correction is well within the uncertainty of our distance measurement from the tangent point to the defining aperture, the corrected distance was used for our irradiance calculation.

D. Stray Light of Spectrometer and Integrating Sphere

Traditionally, the slit-scattering function is used to describe the contribution of stray light to the measured signal for a spectrometer system and to correct

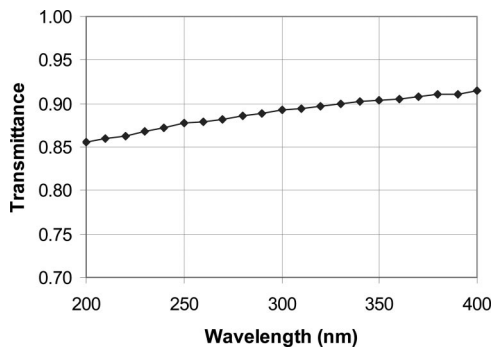


Fig. 5. Typical result of a transmittance measurement of the fused silica window at the FICUS.

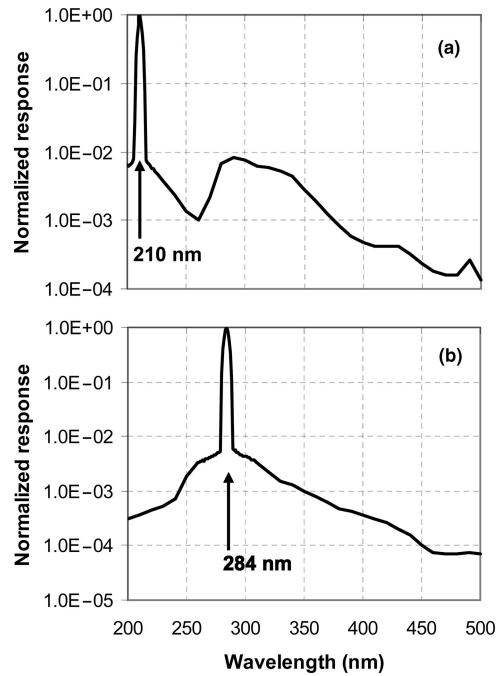


Fig. 6. Measured slit-scattering function of the integrating sphere and spectrometer system with laser wavelengths at (a) 210 nm and (b) 284 nm. Note the fluorescence peak near 300 nm with 210 nm laser light originated from the integrating sphere.

the measured signal from spurious stray-light contributions using the algorithm described in Section 2. A straightforward technique for measuring the slit-scattering function is to use a narrowband tunable source, such as a laser, to irradiate the spectrometer.

For UV work involving integrating spheres as in this work, we found that an additional stray-light contribution could be in the form of fluorescence from the integrating sphere made of PTFE. A detailed dis-

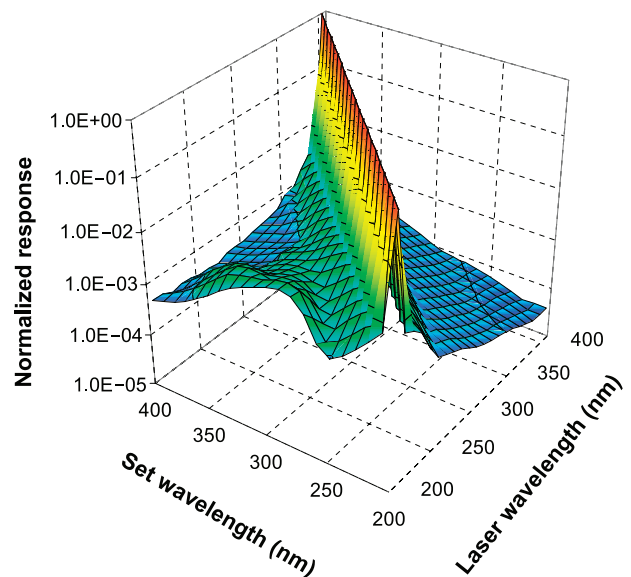


Fig. 7. Measured slit-scattering function of the integrating sphere and spectrometer system.

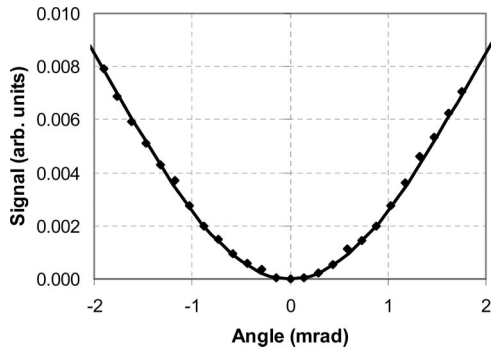


Fig. 8. Vertical scan with polarizer at 350 nm to determine on-orbit position. The solid curve is the fitted curve calculated from the Schwinger equation with only a vertical polarization component.

discussion of the dependence of fluorescence on the conditions of the sphere materials will be presented elsewhere. For this work, we found that, mathematically, the fluorescence effect could be treated the same way as the stray light in the spectrometer, and a single slit-scattering function, $z(\lambda_1, \lambda_2)$, could be used to describe both phenomena. Therefore all the measurements of the slit-scattering function were performed with the integrating sphere and the spectrometer as a single system.

To measure the slit-scattering function, we used UV radiation from the tunable lasers at the NIST facility of the spectral irradiance and radiance responsivity calibrations using uniform sources (SIRCUS).³⁹ A fixed wavelength laser beam from 200 to 400 nm irradiated the integrating sphere and spectrometer system while the wavelength of the spectrometer was scanned, and the resulting signal was recorded. Figure 6 depicts two measurements performed with two laser wavelengths, 210 and 284 nm. With 284 nm, the decaying wings on both sides of the incident wavelength represent the contribution from stray light inside the spectrometer. However, with 210 nm, the result shows a clear flu-

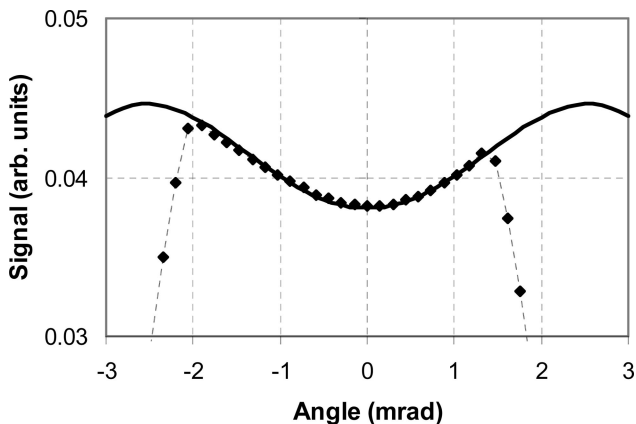


Fig. 9. Same as in Fig. 8 but without the polarizer. The fitted curve is calculated from the Schwinger equation with contribution from both polarization states. The sharp decrease in measurement at the large angle is from the shadowing of the baffle system.

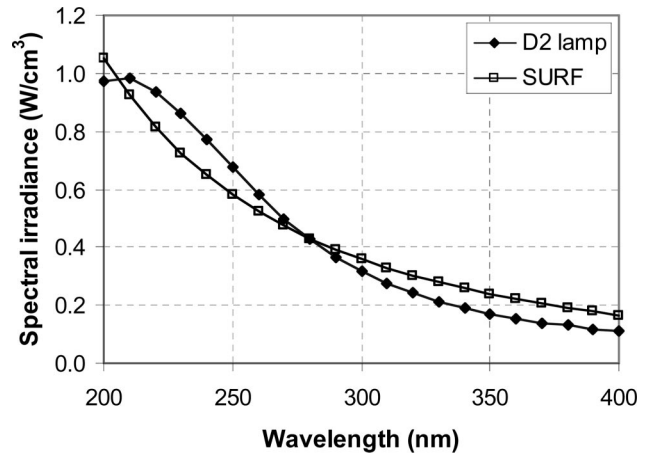


Fig. 10. Comparison of spectral irradiance from a typical deuterium lamp at 30 cm from the source and from SURF III, which is calculated with 380 MeV electron energy and 15 mA of electron beam current. The calculated and measured data points are connected by lines to guide the eye.

orescence peak near 300 nm that was excited from the walls of the integrating sphere by the 210 nm laser beam. In Fig. 7 we illustrate the slit-scattering function of the integrating sphere and spectrometer system measured with a range of laser wavelengths from 200 to 400 nm.

E. Determination of Orbital Plane Position

Unlike blackbody sources, synchrotron radiation is not uniform in the vertical direction (i.e., the direction perpendicular to the electron orbital plane). To assure accuracy in the calculated flux entering an aperture, the positioning of the aperture relative to the orbital plane is crucial. For this work, a preferred position for the defining aperture is on the orbital plane with $\psi = 0$ where, at SURF III with a typical electron energy of 380 MeV, synchrotron radiation from 200 to 400 nm has a local minimum with only horizontally polarized radiation present. As ψ increases above or below the orbital plane, the

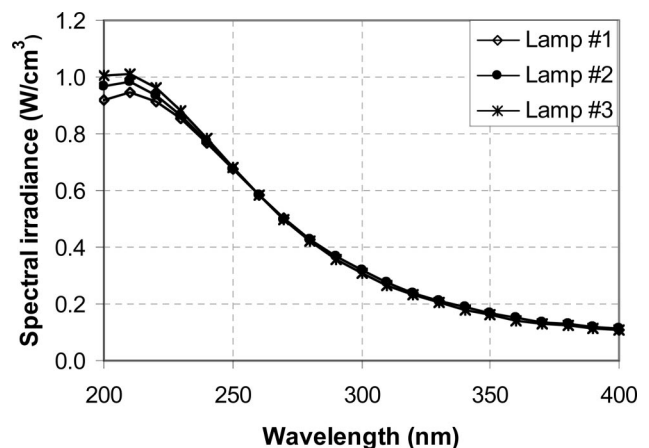


Fig. 11. Spectral irradiance of three deuterium lamps calibrated at the FICUS. Data points are connected by lines to guide the eye.

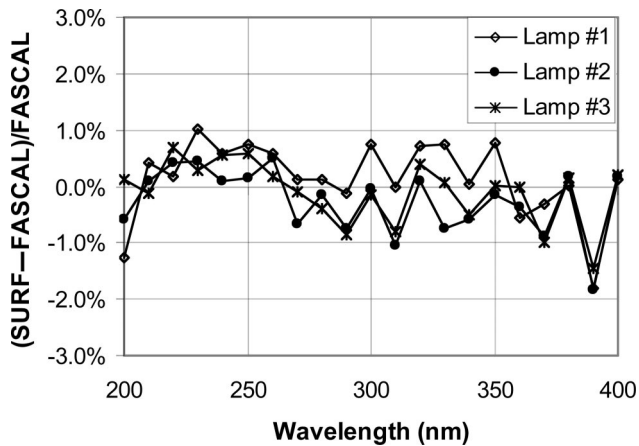


Fig. 12. Percentage differences between the spectral irradiance measured at SURF and at FASCAL for three deuterium lamps.

contribution from vertically polarized radiation increases, and the total flux increases. We used this characteristic angular distribution to determine the on-orbit position for our detector system.

Angular distribution measurements were performed by vertical scans of the spectrometer and detector system with two configurations. In the first configuration, a polarizer was mounted in front of the aperture to allow only vertically polarized radiation into the integrating sphere. Figure 8 shows the result of such a scan at 350 nm and the fitted curve calculated from the vertical polarization component of the Schwinger equation. The on-orbit position was determined as the minimum position where the synchrotron radiation was completely horizontally polarized. In the second configuration, the polarizer was removed from the aperture such that the total flux from both polarization states could be measured. The result is illustrated in Fig. 9 along with the fitted curve calculated from the Schwinger equation. The on-orbit position can again be found at the minimum for this wavelength. The on-orbit position determined by both configurations was in good agreement.

Finally, one should note that the good agreement between measurement and the fitted curve in Fig. 9 indicates excellent depolarization by the integrating

sphere. This is because the spectrometer's throughput is very sensitive to the polarization, and if the radiation entering the spectrometer has any remnant polarization, then the response of the system will be different for two polarization states resulting in a deviation from the calculated angular distribution.

5. Calibration Results at FICUS

In the UV, deuterium lamps have long been used as transfer standards⁴⁰ because of their high and mostly continuum UV radiant power, low visible and IR emission, compact size, and low cost. Similar to synchrotron radiation from SURF III, the emission spectrum of deuterium lamps above 200 nm decreases with longer wavelength as shown in Fig. 10. The striking spectral resemblance between the two sources from 200 to 400 nm is a great advantage in calibrating deuterium lamps directly against synchrotron radiation.

Recently, commercial deuterium lamps with good stability have been identified.⁴¹ These lamps, with long-term relative stability of the intensity of $\sim 10^{-4} \text{ h}^{-1}$ and ignition reproducibility of $\sim 10^{-3}$, were used as transfer standards for the international intercomparison of spectral irradiance from 200 to 360 nm organized by the Comité Consultatif de Photométrie et Radiométrie (CCPR-K1b intercomparison).⁴¹ We have calibrated three of the deuterium lamps at the FICUS.

The irradiance calibrations of all three lamps were performed with the receiving aperture of the integrating sphere at a distance of 30 cm from a reference plane on the housing of the lamps. The reference plane was defined by the front surface of a cap that could be attached to the front of the housing. The center of the glass and its normal also defined the center and viewing angle of the lamps, which was aligned by using a laser. Each lamp had at least 40 min warm-up time before a measurement was performed by the spectrometer and detector system. After the measurement with a lamp, the spectrometer-detector system was moved to measure synchrotron radiation. This measurement was typically performed with an electron beam current of approximately 15 mA such that the irradiance was comparable for both sources. To check repeatability, several rounds of measurements with both sources

Table 1. Components of the Relative Uncertainty ($k = 2$) of Spectral Irradiance of Synchrotron Radiation at the FICUS

Source of Uncertainty	Nominal Value	Relative Uncertainty	Sensitivity Coefficient	Uncertainty in Irradiance
Electron energy	380 MeV	0.02%	0.057	0.0011%
Beam current	~ 15 mA	0.4%	1	0.4%
Orbital radius	83.70773 cm	10^{-10}	0.66	6.6×10^{-11}
Window transmittance	~ 0.8	0.5%	1	0.5%
Distance	692.6 cm	0.086%	2.0	0.17%
Detector alignment		$\pm 0.6 \text{ mm}^2$	0.0011	0.066%
Aperture size	0.95 cm	6.3%	0.015	0.096%
Air absorption ^b			1	0.24%
Combined				0.72%

^aAbsolute uncertainty.

^bFor wavelengths below 205 nm, $<0.1\%$ for wavelengths longer than 205 nm.

Table 2. Components of the Relative Uncertainty ($k = 2$) of Spectral Irradiance of Deuterium Lamp Calibration at the FICUS

Source of Uncertainty	Nominal Value	Relative Uncertainty	Sensitivity Coefficient	Uncertainty in Irradiance
SURF radiation			1	0.72%
Wavelength		$\pm 0.1 \text{ nm}^a$	0.013	0.27%
Stray light and fluorescence			1	0.5%
Lamp distance	30 cm	0.066%	2.0	0.13%
Lamp stability			1	0.5%
Random uncertainty			1	0.6%
Combined				1.2%

^aAbsolute uncertainty.

were performed. Finally, the transmittance of the window in the beamline was measured using the technique discussed in Section 4. Figure 11 displays the measured spectral irradiance of all three lamps based on the scale of SURF III radiation.

To compare the SURF irradiance scale with the irradiance scale maintained at FASCAL, the three deuterium lamps were also calibrated at FASCAL. The variation in measured spectral irradiance between the two facilities is shown in Fig. 12 with agreement well within the relative measurement uncertainty of FASCAL at approximately 4% ($k = 2$).¹⁴

6. Measurement Uncertainty Analysis

The uncertainty in irradiance measurement at the FICUS consists of two parts: first, the uncertainty of the primary synchrotron-radiation-based irradiance scale, and second, the overall uncertainty for calibrating a DUT source, such as a deuterium lamp. The first part correlates with the measurement uncertainties in SURF and beamline parameters as discussed in Section 4. The second part is the combined uncertainty from the primary scale, the transfer of the irradiance scale, and the source's lighting and aging characteristics.

The uncertainty of the primary synchrotron-radiation-based irradiance scale is the uncertainty in predicting the spectral irradiance of the synchrotron radiation inside the defining aperture. The calculated irradiance is directly proportional to some of the parameters (i.e., the sensitivity coefficient is equal to 1), such as electron beam current and window transmission, while other parameters, such as electron energy and electron beam orbital radius, have a nonlinear relationship with the irradiance. For the latter parameters, the sensitivity coefficients were calculated numerically by varying each parameter and finding the amount of change in the resulting irradiance. Table 1 lists the estimated components of the primary scale uncertainty. The combined relative uncertainty for the primary scale of the FICUS is 0.7% ($k = 2$), with the largest contribution coming from the electron beam current and window transmittance.

The same technique was used to analyze the uncertainties in the measurement of the spectral irradiance from a deuterium lamp as listed in Table 2. The relative combined uncertainty of 1.2% ($k = 2$) is

much lower than the more than 4% ($k = 2$) uncertainty for the gas-arc lamp-based scale used at FASCAL from 200 to 250 nm. For longer wavelengths, the improvement in uncertainty at the FICUS is caused mainly by the more stable deuterium lamps used as transfer standards for this work.

7. Conclusions and Outlook

We have built a new facility, the FICUS, for spectral irradiance calibrations in the UV with improved uncertainties over the current disseminated NIST scale. FICUS complements the current irradiance scale based on blackbody sources and covers a wide UV region that is beyond reach with blackbody sources. The primary scale of the facility is based on synchrotron radiation from SURF III through a white-light beamline with only one vacuum window to preserve the calculability of the radiation. A novel technique was used to measure the transmittance of the window *in situ* instead of having to remove the window from the beamline for measurement elsewhere. The system for detecting the radiation was characterized by using tunable lasers for the stray light in the spectrometer and the fluorescence from the integrating sphere. A stray-light reduction algorithm was used to correct the measured signal from synchrotron radiation and radiation from DUT sources.

We have performed spectral irradiance calibrations of a set of deuterium lamps by using this facility with an estimated relative uncertainty of 1.2% ($k = 2$) from 200 to 400 nm. The results were compared with separate measurements at FASCAL with good agreement, well within the uncertainties of both facilities. At present, the FICUS calibrations are limited to the air-UV wavelength region. An upgrade is already under way to evacuate all beam paths and to expand the calibration capability to below 200 nm. In the near future, the FICUS will provide a broad spectral range for the radiometric community from the vacuum UV to the air UV.

The authors thank SURF staff members Alex Farrell, Mitchell Furst, and Edward Hagley for operation of the synchrotron that made this work possible. They also thank Charles Clark for his continuing support of this project.

References

1. A. C. Parr, R. U. Datla, J. L. Gardener, eds., *Optical Radiometry*, Vol. 41 of Experimental Methods in the Physical Sciences (Elsevier, 2005).
2. R. Stair, R. G. Johnson, and E. W. Halback, "Standard of spectral radiance for the region of 0.25 to 2.6 microns," *J. Res. Natl. Bur. Stand. (U.S.)* **64A**, 291–296 (1960).
3. R. Stair, W. Schneider, and J. K. Jackson, "A new standard of spectral irradiance," *Appl. Opt.* **2**, 1151–1154 (1963).
4. W. R. Ott, P. Fieffe-Prevost, and W. L. Wiese, "VUV radiometry with hydrogen arcs. 1: Principle of the method and comparisons with blackbody calibrations from 1650 Å to 3600 Å," *Appl. Opt.* **12**, 1618–1629 (1973).
5. W. R. Ott, K. Behringer, and G. Gieres, "Vacuum ultraviolet radiometry with hydrogen arcs. 2: The high power arc as an absolute standard of spectral irradiance from 124 nm to 360 nm," *Appl. Opt.* **14**, 2121–2128 (1975).
6. J. M. Bridges and W. R. Ott, "Vacuum ultraviolet radiometry. 3: The argon mini-arc as a new secondary standard of spectral radiance," *Appl. Opt.* **16**, 367–376 (1977).
7. D. Stuck and B. Wende, "Photometric comparison between two calculable vacuum-ultraviolet standard radiation sources: synchrotron radiation and plasma-blackbody radiation," *J. Opt. Soc. Am.* **62**, 96–100 (1972).
8. D. H. Tombouljian and P. L. Hartman, "Spectral and angular distribution of ultraviolet radiation from the 300 MeV Cornell synchrotron," *Phys. Rev.* **102**, 1423–1447 (1956).
9. K. Codling and R. P. Madden, "Characteristics of the 'synchrotron light' from the NBS 180 MeV machine," *J. Appl. Phys.* **36**, 380–387 (1965).
10. G. Bathow, E. Freytag, and R. Haensel, "Measurement of synchrotron radiation in the x-ray region," *J. Appl. Phys.* **37**, 3449–3454 (1966).
11. D. Lemke and D. Labs, "The synchrotron radiation of the 6 GeV DESY machine as a fundamental radiometric standard," *Appl. Opt.* **6**, 1043–1048 (1967).
12. E. Pitz, "Absolute calibration of light sources in the vacuum ultraviolet by means of the synchrotron radiation of DESY," *Appl. Opt.* **8**, 255–259 (1969).
13. J. H. Walker, R. D. Saunders, and A. T. Hattenburg, *Spectral Radiance Calibration*, NBS Special Publication 250-1 (National Bureau of Standards, 1987).
14. J. H. Walker, R. D. Saunders, J. K. Jackson, and D. A. McSparron, *Spectral Irradiance Calibration*, NBS Special Publication 250-20 (National Bureau of Standards, 1987).
15. J. Schwinger, "On the classical radiation of accelerated electrons," *Phys. Rev.* **75**, 1912–1925 (1949).
16. D. L. Ederer, E. B. Saloman, S. C. Ebner, and R. P. Madden, "The use of synchrotron radiation as an absolute source of VUV radiation," *J. Res. Natl. Bur. Stand. (U.S.)* **79A**, 761–774 (1975).
17. P. J. Key and T. H. Ward, "The establishment of ultraviolet spectral emission scales using synchrotron radiation," *Metrologia* **14**, 17–29 (1978).
18. T. Zama and I. Saito, "Calibration of absolute spectral radiation in UV and VUV regions by using synchrotron radiation," *J. Electron Spectrosc. Relat. Phenom.* **144–147**, 1087–1091 (2005).
19. M. Stock, J. Fischer, R. Freidrich, H. J. Jung, R. Thornagel, G. Ulm, and B. Wende, "Present state of the comparison between radiometric scales based on three primary standards," *Metrologia* **30**, 439–449 (1993).
20. F. Lei, W. Paustian, and E. Tegeler, "Determination of the spectral radiance of transfer standards in the spectral range 110 nm to 400 nm using BESSY as a primary source standard," *Metrologia* **32**, 589–592 (1995).
21. M. Richter, J. Hollandt, U. Kroth, W. Paustian, H. Rabus, R. Thornagel, and G. Ulm, "Source and detector calibration in the UV and VUV at Bessy II," *Metrologia* **40**, S107–S110 (2003).
22. L. R. Hughey and A. R. Schaefer, "Reduced absolute uncertainty in the irradiance of SURF-II and instrumentation for measuring linearity of x-ray, XUV and UV detectors," *Nucl. Instrum. Methods Phys. Res.* **195**, 367–370 (1982).
23. A. R. Schaefer, L. R. Hughey, and J. B. Fowler, "Direct determination of the stored electron beam current at the NBS electron storage ring, SURF-II," *Metrologia* **19**, 131–136 (1984).
24. A. R. Schaefer, R. D. Saunders, and L. R. Hughey, "Intercomparison between independent irradiance scales based on silicon photodiode physics, gold-point blackbody radiation, and synchrotron radiation," *Opt. Eng.* **25**, 892–896 (1986).
25. H. J. Kostkowski, J. L. Lean, R. D. Saunders, and L. R. Hughey, "Comparison of the NBS SURF and tungsten ultraviolet irradiance standards," *Appl. Opt.* **25**, 3297–3306 (1986).
26. J. L. Lean, H. J. Kostkowski, R. D. Saunders, and L. R. Hughey, "Comparison of the NIST SURF and argon miniarc irradiance standards at 214 nm," *Appl. Opt.* **28**, 3246–3253 (1989).
27. A. Thompson, E. A. Early, and T. R. O'Brian, "Ultraviolet spectral irradiance scale comparison: 210 nm to 300 nm," *J. Res. Natl. Inst. Stand. Technol.* **103**, 1–13 (1998).
28. U. Arp, R. Friedman, M. L. Furst, S. Makar, and P.-S. Shaw, "SURF III—an improved storage ring for radiometry," *Metrologia* **37**, 357–360 (2000).
29. P.-S. Shaw, D. Shear, R. J. Stamilio, U. Arp, H. W. Yoon, R. D. Saunders, A. C. Parr, and K. R. Lykke, "The new beamline 3 at SURF III for source-based radiometry," *Rev. Sci. Instrum.* **73**, 1576–1579 (2002).
30. P.-S. Shaw, U. Arp, H. W. Yoon, R. D. Saunders, A. C. Parr, and K. R. Lykke, "A SURF beamline for synchrotron source-based absolute radiometry," *Metrologia* **40**, S124–S127 (2003).
31. J. D. Jackson, *Classical Electrodynamics*, 2nd ed. (Wiley, 1975), Chap. 14.
32. H. J. Kostkowski, *Reliable Spectroradiometry* (Spectroradiometry Consulting, 1997), Chap. 4.
33. S. W. Brown, B. C. Johnson, M. E. Feinholz, M. A. Yarbrough, S. J. Flora, K. R. Lykke, and D. K. Clark, "Stray-light correction algorithm for spectrographs," *Metrologia* **40**, S81–S84 (2003).
34. Y. Zong, S. W. Brown, B. C. Johnson, K. R. Lykke, and Y. Ohno, "Simple spectral stray light correction method for array spectroradiometers," *Appl. Opt.* **45**, 1111–1119 (2006).
35. P.-S. Shaw, R. Gupta, and K. R. Lykke, "Characterization of an ultraviolet and vacuum-ultraviolet irradiance meter with synchrotron radiation," *Appl. Opt.* **41**, 7173–7178 (2002).
36. P.-S. Shaw, R. Gupta, and K. R. Lykke, "Stability of photodiodes under irradiation with a 157-nm pulsed excimer laser," *Appl. Opt.* **44**, 197–207 (2005).
37. P.-S. Shaw, U. Arp, and K. R. Lykke, "Absolute radiant flux measurement of the angular distribution of synchrotron radiation," *Phys. Rev. ST Accel. Beams* **9**, 070701 (2006).
38. G. P. Eppeldauer and J. E. Hardis, "Fourteen-decade photocurrent measurements with large-area silicon photodiodes at room temperature," *Appl. Opt.* **30**, 3091–3099 (1991).
39. S. W. Brown, G. P. Eppeldauer, and K. R. Lykke, "NIST facility for spectral irradiance and radiance responsivity calibrations with uniform sources," *Metrologia* **37**, 579–582 (2000).
40. R. D. Saunders, W. R. Ott, and J. M. Bridges, "Spectral irradiance standard for the ultraviolet: the deuterium lamp (E)," *Appl. Opt.* **17**, 593–600 (1978).
41. P. Sperfeld, K. D. Stock, K.-H. Raatz, B. Nawo, and J. Metzendorf, "Characterization and use of deuterium lamps as transfer standards of spectral irradiance," *Metrologia* **40**, S111–S114 (2003).